Ultrastructure of Hybrid Chitosan–Glycerol Phosphate Blood Clots by Environmental Scanning Electron Microscopy

M. ILIESCU,[1] C.D. HOEMANN,[1] M.S. SHIVE,[2] A. CHENITE,[2] AND M.D. BUSCHMANN[1]*
[1]*Department of Chemical Engineering, Institute of Biomedical Engineering, Ecole Polytechnique, Montreal, Quebec, Canada H3C 3A7*
[2]*BioSyntech Canada Inc., 475 Blvd. Armand Frappier, Laval, Quebec, H7V 4B3 Canada*

KEY WORDS chitosan; chitosan–glycerol phosphate; biomaterials; blood; glutaraldehyde; paraformaldehyde; environmental scanning electron microscopy; cartilage repair; arthritis

ABSTRACT Chitosan-based polymers have been extensively studied for biomedical applications. Recently, liquid solutions of chitosan in a glycerol phosphate buffer (chitosan–GP) with physiological pH and osmolality were mixed with autologous blood to form hybrid chitosan–GP/blood implants that improved the repair of articular cartilage lesions in a large animal model. The mixture of chitosan–GP and blood forms a viscous liquid, which solidifies in minutes via normal blood coagulation as well as chitosan-mediated mechanisms. Here we have examined the ultrastructure of these chitosan–GP/blood clots as well as regular blood clots and chitosan–GP gels, the latter produced by heating. Both unfixed and fixed samples of chitosan–GP/blood clots, regular blood clots, and chitosan–GP gels were investigated by environmental scanning electron microscopy (ESEM) in conjunction with energy dispersive X-ray spectrometry (EDS), the former permitting direct observation of the ultrastructure in hydrated conditions simulating the natural state. By examination of unfixed specimens using ESEM we found that chitosan formed a network structure in both chitosan–GP gels and chitosan–GP/blood clots; however this structure was altered by aldehyde fixation to produce artifactual aggregates of chitosan microparticles. We were also able to identify chitosan in chitosan–GP/blood clots by washing samples in low concentration NaCl solutions followed by local EDS analyses to identify excess chloride versus sodium, and thus presence of cationic chitosan in analyzed features. Additional results indicated that the majority of glycerol phosphate diffuses freely from chitosan–GP gels (by EDS of phosphorus) and that hyperosmotic paraformaldehyde-based fixatives (i.e. 4% w/v) significantly disturb erythrocyte morphology in fixed whole blood clots. *Microsc. Res. Tech. 71:236–247, 2008.*

INTRODUCTION

Wound healing in vascularized tissues is triggered by the formation of a blood clot that reestablishes haemostasis, generates cell recruitment, and serves as a scaffold for invading repair cells (Clark, 1996; Colman et al., 2001). However, adult articular cartilage, the nearly frictionless load-bearing material covering the ends of bones in joints, has an intrinsically low capacity for repair when damaged (Tallheden et al., 2003), primarily due to its avascular nature. Many orthopedic surgical approaches have attempted to aid cartilage repair including allogenic grafts, autologous cell-based therapy, and a family of surgical techniques termed bone-marrow stimulation (Buckwalter and Mankin, 1998). In the latter category, damaged cartilage lesions are debrided to expose subchondral bone, which is then microfractured or drilled to access marrow blood and induce a bone-derived repair response. Unfortunately, this response is limited due to the poor retention of the blood clot formed on the bone surface in these cartilage lesions and the subsequent platelet-mediated contraction of the clot.

One approach to improve healing is to stabilize the blood clot by dispersing a soluble biocompatible polymer throughout uncoagulated fresh blood. The polymer acts as a scaffold throughout the clot to maintain its volume and to increase clot adhesion to cartilaginous and osseous surfaces at the lesion site. Ideally, the polymer should be soluble at physiological pH and osmolarity, as well as nontoxic and bioresorbable, in addition to permitting coagulation and impeding clot retraction. Such a system has been developed using chitosan, a linear aminopolysaccharide with interspersed units of D-glucosamine and acetyl-D-glucosamine, that is solubilized in an aqueous glycerol phosphate (GP) solution termed chitosan–GP (Chenite et al., 2000, 2001; Filion et al., 2007; Hoemann et al., 2005a; Zan et al., 2006; Lavertu et al., 2007). A specific chitosan–GP solution (called BST-CarGel™) can be

*Correspondence to: M.D. Buschmann, Department of Chemical Engineering, Institute of Biomedical Engineering, Ecole Polytechnique, Montreal, Quebec, Canada H3C 3A7. E-mail: Michael.buschmann@polymtl.ca

Received 27 June 2007; accepted in revised form 3 October 2007

Contract grant sponsors: Canadian Institutes of Health Research (CIHR), The Canadian Foundation for Innovation (CFI), The Natural Sciences and Engineering Research Council of Canada (NSERC), The Canada Research Chairs Program, BioSyntech Canada Inc.

DOI 10.1002/jemt.20545

Published online 27 November 2007 in Wiley InterScience (www.interscience.wiley.com).

mixed with autologous blood to form viscous chitosan–GP/blood mixtures that solidifies in about 10 min, in part due to the thrombogenicity of chitosan (Hoemann et al., 2006). A whole blood clot quickly looses a great extent of its volume via clot retraction; a platelet-mediated contractile process that exudes serum (Cohen et al., 1982; Morgenstern et al., 1990; White, 2000). In contrast, chitosan–GP/blood clots do not retract, but rather maintain their volume after coagulation (Hoemann et al., 2006). In addition to maintaining clot volume and enhanced adhesion to cartilage and bone surfaces, chitosan–GP/blood clots may help extend the activity of growth factors that are beneficial for wound repair. We have previously found that application of these physically stabilized chitosan–GP/blood clots to marrow-stimulated cartilage defects result in increased quantity and hyaline quality of repair cartilage in adult sheep and rabbit animal models (Chevrier et al., 2006; Hoemann et al., 2005b, 2006). Chitosan–GP solutions were previously found to induce red blood cell chaining during coagulation (Hoemann et al., 2007), however the manner in which chitosan interacts with blood components in solidified hybrid chitosan–GP/blood clots and resulting ultrastructure has not been elucidated.

In general, to allow ultrastructural investigation of cells and tissues, samples are treated with preservatives and fixatives. Formaldehyde (CH_2O) as 4% v/v buffered formaldehyde (that is equivalent to 10% buffered formalin) is the most widely employed fixative (Hayat, 2000; Hunter, 1993). A particular form of formaldehyde is paraformaldehyde [(—CH_2O—)n], also called polyoxymethylene, that is a solid state high molecular weight polymerized formaldehyde (Sheehan and Hrapchak, 1987). Paraformaldehyde crosslinks proteins to create a gel matrix that preserves certain in vivo constituents and their interactions (Leong, 1994). Glutaraldehyde [$OHC(CH_2)_3CHO$], another common fixative (Hayat, 2000; Sheehan and Hrapchak, 1987; Hunter, 1993), is a dialdehyde that rapidly reacts with proteins and forms stabilized structures by crosslinking. With aldehydes, crosslinks are predominantly formed between proteins mostly involving the basic amino acid lysine, although other groups such as imino, amido, hydroxyl, carboxyl, sulfydryl, guanidyl, peptide, or aromatic rings may also be involved (Leong, 1994). In terms of strength of fixation, paraformaldehyde provides less stability than glutaraldehyde, the latter believed to be the best structural preservative since its extensive fixation is quite robust. Fixatives containing both paraformaldehyde and glutaraldehyde are also employed since they can provide certain advantages compared with either alone (Hayat, 2000).

The objective of this study was to characterize the structure and relationships of the various components of chitosan–GP/blood clots compared with chitosan–GP gels alone and clots containing whole blood-only. We used environmental scanning electron microscopy (ESEM) (Danilatos, 1981a) in conjunction with energy dispersive X-ray analysis (EDS) to investigate the structural and compositional details of different samples, including the morphology of cells, chitosan-specific structures, and fibre components. The high water vapour pressure in the ESEM analysis chamber allows high resolution imaging at levels of relative humidity representing wet or hydrated specimens, obviating the need for sample drying and the associated artefacts (Muscariello et al., 2005). Relative humidity can also be controlled by manipulation of the temperature and pressure within the ESEM chamber (Danilatos, 1981b). We further examined the influence of different formulations of aldehyde-based fixatives and washing treatments on the structure, architecture, and organization of chitosan–GP gels, chitosan–GP/blood clots and whole blood clots.

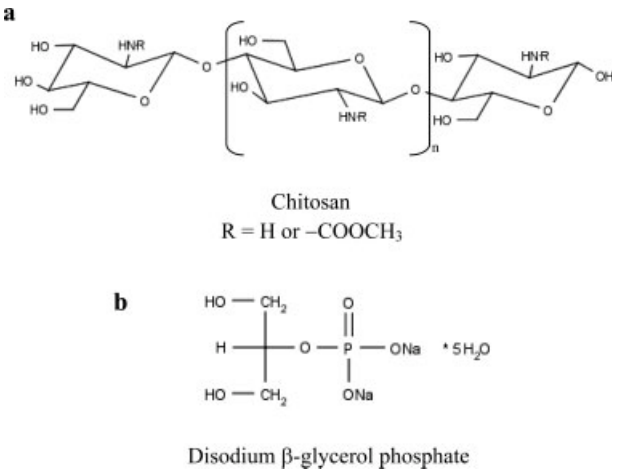

Fig. 1. Structure of disodium β-glycerol phosphate and chitosan.

MATERIALS, METHODS, AND EXPERIMENTAL PROTOCOLS

Chitosan Solutions, Glycerol Phosphate (GP) Solutions, and Chitosan–GP Gels

Sterile aqueous solutions of ultrapure chitosan (Fig. 1a) with degree of deacetylation (DDA) of 81.7(±3)% and average molecular weight of 320 kDa (by triple detector gel permeation chromatography) were provided (BioSyntech Canada, Laval, Qc, Canada) at 2.09% (wt/wt) chitosan concentration with 75 mM HCl, corresponding to ~80% (mol/mol) of Cl^- per chitosan total amine (NH_2 + NH_3^+) groups. The pH of this solution was 5.81 and the apparent viscosity 1369 mPa s (at 25°C, Brookfield viscometer LVDVI+, Brookfield Engineering Laboratories, Middleboro, MA). Disodium β-glycerol phosphate (GP, $C_3H_7Na_2O_6P$, Fig. 1b) was provided (BioSyntech Canada, Laval, Qc, Canada) at 0.5 M (10.19% wt/wt) concentration with 50 mM of HCl to obtain a pH of 6.99. Chitosan–GP solutions (BST-CarGel™, BioSyntech) for mixing with blood (see below) were prepared by adding 0.3 mL of the GP solution to 1.18 mL of the chitosan solution to create a chitosan–GP solution with 1.67% wt/wt chitosan, 101 mM GP, 70 mM HCl at pH 6.8. To study the structure of chitosan–GP without blood, a greater quantity of the GP solution, namely 0.6 mL, was added to 1.18 mL chitosan to create a thermogelling chitosan–GP solution (Chenite et al., 2000) with 1.39% wt/wt chitosan, 168 mM GP, 67 mM HCl at pH 6.8. This solution was gelled by heating at 50°C for 60 min.

TABLE 1. Composition, osmolality, and pH of fixatives used

No.	Fixative	Osmolality—experimental (mOsm/kg)	Osmolality—calculated (mOsm/kg)	pH
1	4% w/v paraformaldehyde + 1% w/v glutaraldehyde, 0.1 M sodium cacodylate	1,657	1,656	7.3
2	4% w/v paraformaldehyde, 0.1 M sodium cacodylate	1,554	1,556	7.3
3	2% w/v paraformaldehyde, 0.1 M sodium cacodylate	870	866	7.3
4	5% w/v glutaraldehyde, 0.1 M sodium cacodylate	763	759	7.3
5	2% w/v glutaraldehyde, 0.1 M sodium cacodylate	431	424	7.3

Preparation of Blood-Only Clots and Chitosan–GP/Blood Clots

To prepare whole blood clots, venous peripheral human blood of healthy nonfasting donors was aseptically withdrawn according to institutional ethics approved procedures, and 0.5 mL of blood was ejected into sterile glass tubes with vented steel caps at 37°C and allowed to clot for 1 h. For chitosan–GP/blood clots, venous peripheral human blood was aseptically withdrawn from donors and 4.5 mL was added to 1.48 mL of chitosan–GP solution (BST-CarGel) in glass vials containing six depyrogenized stainless steel mixing beads (0.39 g each, Salem Specialty Ball Co, Canton, CT) and shaken vigorously (50 times) during 10 s. Seven aliquots of 0.2 mL were then distributed to glass tubes and allowed to solidify at 37°C for 1 h.

Fixation Solutions and Sample Fixation and Processing Prior to Imaging Analysis

Five distinct fixation solutions using glutaraldehyde and paraformaldehyde were used (Table 1) to evaluate the effect of fixation and potential fixation artefacts on observed sample ultrastructure. All fixatives were prepared in sodium cacodylate ($(CH_3)_2AsO_2Na$, Fisher Scientific, St-Laurent, Qc, Canada) buffer as this is known to be beneficial for ultrastructural preservation (Leong, 1994) and also permits unambiguous identification of GP by phosphate detection in EDS (see ESEM and EDS Investigation). The pH was stabilized at 7.3 by drop-wise addition of 6 N HCl. The fixative osmolality was measured by freezing point depression, extrapolated from samples diluted 1:4 in ddH_2O, using an Advanced Osmometer Model 3D3 (Advanced Instruments, Norwood, MA) (Table 1). The theoretical osmolality of fixatives and sodium cacodylate buffer was also calculated using the following equations assuming an ideal dilute solution where the osmotic coefficient $\Phi = 1$ and approximating the mass concentration of H_2O in solution as 1 kg/L, thereby neglecting the diluting effect of solutes.

(i). $(\text{Solute})_i$ molality (mmol/kg) = $(\text{Solute})_i$ molarity (mmole/L)/H_2O concentration (1 kg/L). i accounts for each solute component dissociating in a given solution.

(ii). Total molality (mmol/Kg) = $\sum_i (\text{Solute})_i$ molality (mmol/kg).

(iii). Total osmolality (mOsm/kg) = $\Phi \times$ Total molality (mmol/kg).

Chitosan–GP samples without blood were allowed to gel at 50°C for 1 h and then fixed with each fixative at 50°C for 2 h (Table 2). Then, fixation solutions were changed and samples were kept overnight at room temperature. The blood-only and chitosan–GP/blood clot samples were first incubated at 37°C for 1 h and then placed in at least 10 vol. of each fixative at room temperature overnight (Table 2). Unfixed samples were kept in glass tubes with vented caps at 37°C prior to subsequent preparation described below.

For chitosan–GP gels, thin strips of about 1 mm thickness were cut from the sample with a clean fresh razor blade. For blood-containing samples (unfixed or fixed), the clots were bisected transversely, then strips of about 1 mm thickness were cut from the halves at about 1/3 of the length of the sample. Before microscopic observation, fixed and unfixed strips were extensively washed 4 times for 30 min by submersion in fresh solutions of ddH_2O or in 10 mM NaCl. Washing was applied to remove any unreacted aldehyde and residues from fixative that could be detrimental to the vacuum pumps system of the microscope. Unfixed strips were also observed without washing. Concentrations of salt higher than 10 mM were found to create crystallized structures on the imaged surface and were therefore avoided (data not shown). All ESEM images were taken from the freshly cut and exposed face. Investigation of different samples was made within as short a time possible following preparation and processing, ~30 min maximum for the unfixed samples.

All samples – chitosan–GP gels, blood-only clots and chitosan–GP/blood clots – were prepared in triplicate. Specimens were observed in at least 3 different sites for each of the chitosan–GP gels for a total of 9 observation sites for the 3 samples, while 10 locations of similar appearance for blood-containing samples were imaged for a total of 30 observation sites. For heterogeneous regions and/or where structural components and detailed features were analyzed, the number of sites of observation was further increased, as needed.

ESEM and EDS Investigation

Samples were observed using an environmental scanning electron microscope (ESEM, Quanta 200 FEG, FEI Company Hillsboro, OR) equipped with an EDS energy dispersive X-ray spectrometer (EDAX, Genesis 2000, XMS System 60 with a Sapphire Si:Li Detector). The instrument has an environmental mode and a low vacuum mode for the examination of hydrated, oily or out-gassing specimens to observe samples in a natural state (Danilatos, 1981a,b). This microscope allows imaging in high vacuum pressure ($\sim 10^{-5}$ Pa) or in the presence of gases and vapors of pressures up to 4,000 Pa in the ESEM mode, without metallic coating (Stokes, 2003; Stokes et al., 2003),

TABLE 2. Chitosan–GP gel samples, gelling conditions, and fixation conditions

Sample	Gelation temperature (°C)	Heating time before fixation (h)	Incubation time at 37°C (h)	Unfixed sample	Fixative					Fixation time at 50°C (h)	Fixation time at room temperature (h)
					4% w/v para + 1% w/v glut	4% w/v para	2% w/vpara	5% w/v glut	2% w/v glut		
Chitosan/HCl/β-GP	50	1	—	√						—	—
Chitosan/HCl/β-GP	50	1	—		√					2	Overnight
Chitosan/HCl/β-GP	50	1	—			√				2	Overnight
Chitosan/HCl/β-GP	50	1	—				√			2	Overnight
Chitosan/HCl/β-GP	50	1	—					√		2	Overnight
Chitosan/HCl/β-GP	50	1	—						√	2	Overnight
Blood-only clot	—	—	—	√						—	—
Blood-only clot	—	—	—		√					—	Overnight
Blood-only clot	—	—	—			√				—	Overnight
Blood-only clot	—	—	—				√			—	Overnight
Blood-only clot	—	—	—					√		—	Overnight
Blood-only clot	—	—	—						√	—	Overnight
Chitosan/HCl/β-GP/blood clot	—	—	1	√						—	—
Chitosan/HCl/β-GP/blood clot	—	—	1		√					—	Overnight
Chitosan/HCl/β-GP/blood clot	—	—	1			√				—	Overnight
Chitosan/HCl/β-GP/blood clot	—	—	1				√			—	Overnight
Chitosan/HCl/β-GP/blood clot	—	—	1					√		—	Overnight
Chitosan/HCl/β-GP/blood clot	—	—	1						√	—	Overnight

using a gaseous secondary electron detector (GSED) (Danilatos, 1983). The microscope employs a field emission tip made of a single crystal tungsten wire sharpened by electrolytic etching of diameter of 10–100 nm and much smaller apparent source size (Rizzieri et al., 2003; Stokes, 2003). The specimen stage is equipped with a Peltier effect temperature controller to permit control of relative humidity by varying temperature and pressure. Global (large scale) and local (spot) EDS analyses were carried out on different sites of samples at accelerating voltages of 5–10 kV. While the incident electron beam spot size is 1–5 nm, the volume of material from which X-rays are generated in local analysis does not exceed 10^5 nm^3 for the accelerating voltage range used. Global analyses were obtained by continuously scanning a given sample surface area, thus representing an accumulation of multiple local analyses. To avoid sample damage by the electron beam, the acquisition time of the recording spectra was kept as short as possible (typically 40 s) but long enough to achieve an acceptable signal/noise ratio. Characteristic emission X-ray lines (specific to each element) appear on the spectra x-axis and X-rays were quantified as counts per seconds (y-axis of spectra). The calibration was performed with standards of Al-Cu alloys that have minimal number of well-known X-ray lines in both lower and higher energy range. Measurements were performed on at least five sites of similar appearance for a given sample. Quantification of elements was done with a relative error per element of ±5% using the Genesis software provided by the manufacturer. Percentages of different elements present in the sample are the mean of measured values in many locations.

Protocols for ESEM Imaging

For blood-containing samples, the pressure in the chamber and the sample temperature were set at 8 Torr and 8°C or 7 Torr and 6°C, respectively, to achieve a relative humidity of water vapor of 100%. After ~2 min of sample stabilization, the pressure was reduced to 2–3.5 Torr to maintain relative humidity at 25–50%. Sample dehydration was therefore avoided, allowing high resolution imaging that revealed details of the supramolecular structure of the blood-containing samples that were distinct from the water surface.

To observe chitosan–GP gels not containing blood a different protocol for sample stabilization and imaging was developed. The pressure was initially set at 4.6 Torr and the temperature just above but very close to 0°C, where according to the phase diagram of water the relative humidity will be 100% (Stokes, 2003). To emphasize the gel microstructure we then decreased the temperature and pressure for 10 min to −5°C and 2–3.5 Torr, respectively, thereby freezing the sample. Subsequently the temperature was allowed to rise at 2°C/min up to 20°C to sublimate water from the sample at a relative humidity of pure water of 12.5–20% at 2–3.5 Torr and 20°C inside the chamber. Without this in situ quasi-lyophilization process, we were unable to observe the microstructure of chitosan–GP gel. This protocol could not be applied to blood-containing samples since freezing distorted cellular structures. It should be noted that the above freezing method does

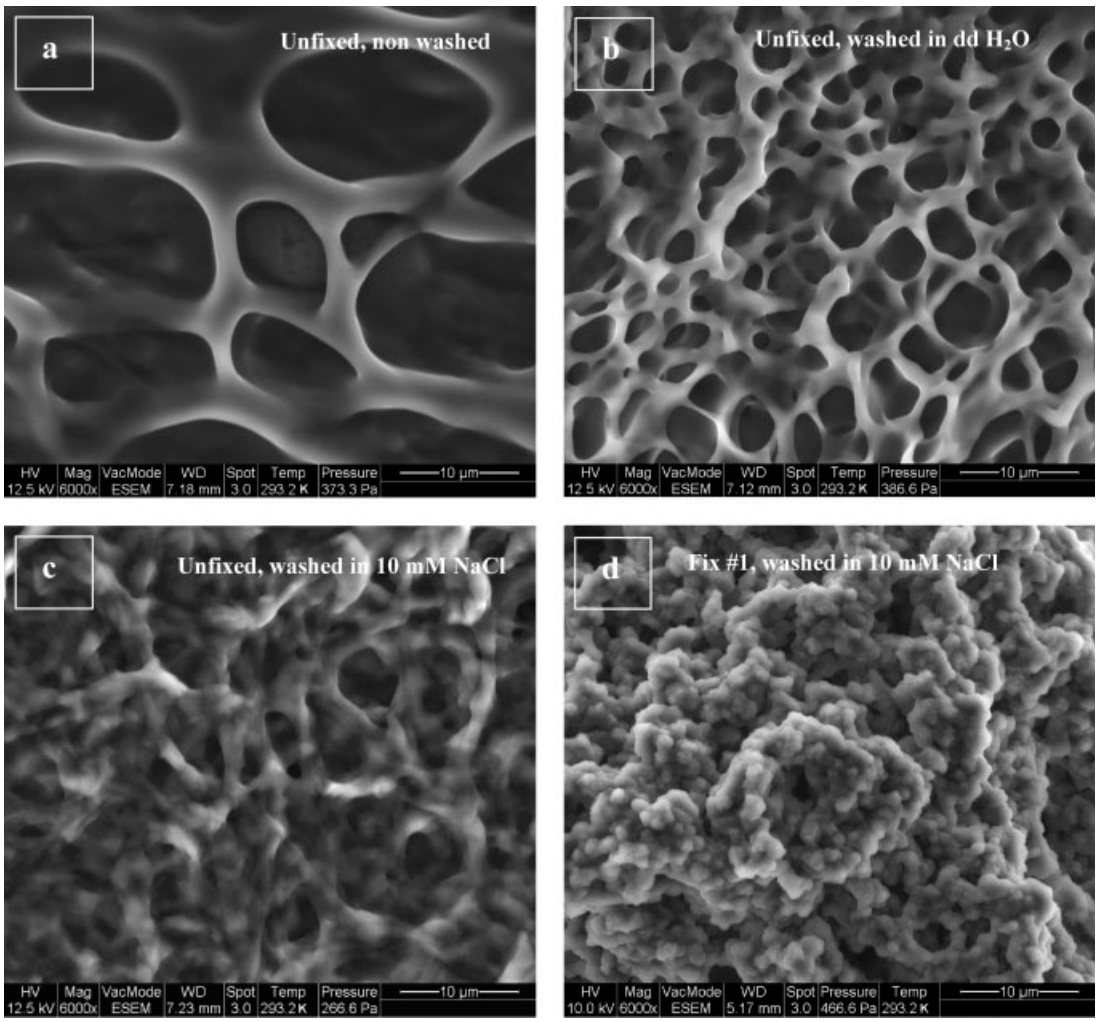

Fig. 2. ESEM images of microstructure of unfixed chitosan–GP gels imaged (**a**) directly without washing (**b**) after washing with distilled and deionized water and (**c**) after washing in 10 mM NaCl aqueous solution and (**d**) ESEM micrograph of a chitosan–GP gel fixed with 4% w/v paraformaldehyde + 1% w/v glutaraldehyde (Fixative no. 1 in Table 1) which produced micron size spherical aggregates, and washed in 10 mM NaCl aqueous solution.

not necessarily confer a sufficiently fast freezing rate to maintain amorphous ice in the bulk. Thus, it is possible eutectic ice phases can form and concentrate other material components to boundaries, although we did not observe this effect.

All images were taken at accelerating voltages of 10–20 kV and working distances of 5–10 mm, depending on the geometrical characteristics, height and surface regularity of the sample.

RESULTS AND DISCUSSION

ESEM Imaging

Unfixed Chitosan–GP Gels and the Effect of Fixatives on Chitosan–GP Gel Ultrastructure. Unfixed chitosan–GP gels retained their gelled state and mechanical consistency throughout the cutting, washing, and ESEM imaging procedure to reveal a uniformly porous mesh-like network structure, with pore sizes ranging from several micrometers up to about 20 μm (Fig. 2). Surrounding the pores, chitosan-containing structures appeared as a continuous network a few micrometers-thick (Fig. 2a). This structure is consistent with that previously reported for lyophilized chitosan–GP gels using conventional SEM (Crompton et al., 2005), where gels were frozen in liquid nitrogen, lyophilized for 24 h and then sputter-coated with gold prior to SEM under high vacuum, resulting in a gel matrix that was partially damaged and cracked. In contrast, our ESEM procedure performs in situ lyophilization, inside the microscope chamber, and obtains a sample with a relative humidity of about 12.5% such specimen damage and artefacts are minimized.

There were significant differences in the morphology comparing unfixed samples imaged without washing to those washed in ddH_2O water and in 10 mM NaCl. Without washing, pores and connecting walls were larger (Fig. 2a) than after washing in water (Fig. 2b) suggesting that washing of the unfixed gel modified pore size and number and the overall microstructure. Samples washed in 10 mM NaCl aqueous solution

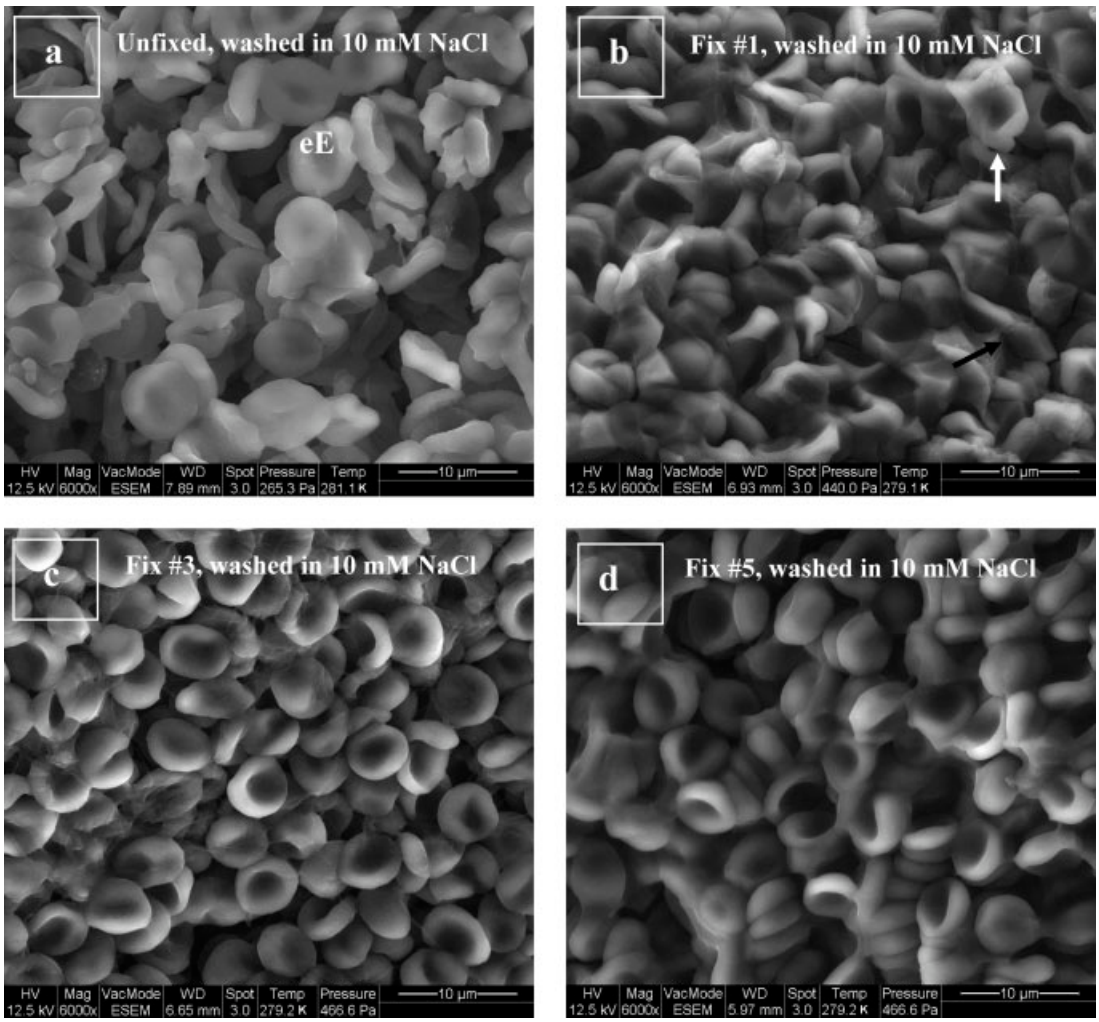

Fig. 3. ESEM images of (**a**) an unfixed blood-only clot washed in 10 mM NaCl and blood-only clots (**b**) fixed with 4% w/v paraformaldehyde mixed with 1% w/v glutaraldehyde (Fixative no. 1 in Table 1) (**c**) 2% w/v paraformaldehyde (Fixative no. 3 in Table 1), and (**d**) 2% w/v glutaraldehyde (Fixative no. 5 in Table 1), all washed with 10 mM NaCl aqueous solution. Erythrocytes morphology is poor when either (a) unfixed or (b) when fixed in hyperosmolar fixatives. eE = expanded erythrocytes, shrunken erythrocyte = white arrows; crushed erythrocytes = black arrows.

became even denser with fewer pores and displaying a highly interconnected branch- and nodular-like meshwork (Fig. 2c) suggesting salt-enhanced precipitation of chitosan at the molecular level.

Fixation of chitosan–GP gels using fixative no. 1 (4% w/v paraformaldehyde + 1% w/v glutaraldehyde, 0.1 M sodium cacodylate) (Table 1) induced a condensed ultrastructure composed of aggregated spherical microparticles of 1.2–1.8 μm in diameter (Fig. 2d). It thus appears that aldehyde-based fixation extensively crosslinks chitosan amino groups and condenses chitosan into microparticles, while conserving a certain degree of porosity between aggregates of these microparticles. We found that the formation of these aggregates of chitosan microparticles occurred with both glutaraldehyde and paraformaldehyde fixation and was independent of the osmolality of the fixative (data not shown).

Unfixed Blood-Only Clots and the Influence of Fixatives on Blood-Only Clots. Whole blood clot samples that were not fixed were difficult to observe in ESEM since they underwent rapid degradation and permanent damage when processed. Among the prepared triplicates only one sample was observable, but it also became irreversibly degraded under the electron beam in less than 1 h. This unfixed sample (Fig. 3a) revealed that most erythrocytes were expanded ("eE" in Fig. 3a).

Whole blood clots that were fixed with aldehyde fixative having the highest osmotic pressure (Fixative no. 1: 4% w/v paraformaldehyde + 1% w/v glutaraldehyde) displayed morphological distortions (Fig. 3b). In particular, most erythrocytes appeared shrunken (white arrows in Fig. 3b) or even effectively crushed (black arrows in Fig. 3b). These distortions are likely caused by the extreme hyperosmolarity of these fixatives of

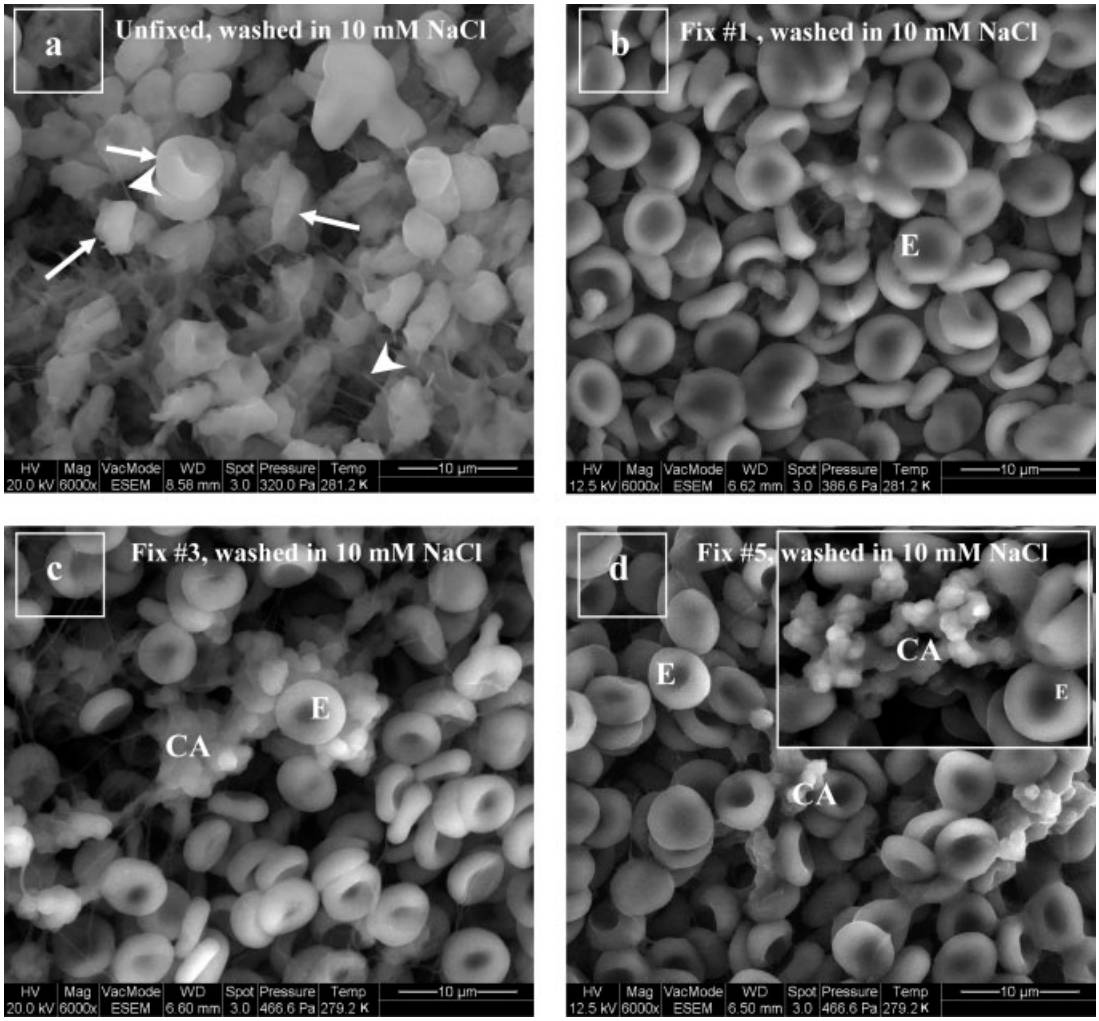

Fig. 4. ESEM images of (**a**) unfixed chitosan–GP/blood clots washed in 10 mM NaCl and (**b**) chitosan–GP/blood-clots fixed with 4% w/v paraformaldehyde + 1% w/v glutaraldehyde (Fixative no. 1 in Table 1) (**c**) 2% w/v paraformaldehyde (Fixative no. 3 in Table 1) and (**d**) 2% w/v glutaraldehyde (Fixative no. 5 in Table 1) all washed in 10 mM NaCl aqueous solution. Inset is a higher magnification of aggregates of chitosan microspheres produced by aldehyde fixatives, using 5% w/v glutaraldehyde (Fixative no. 4 in Table 1) as an example. White arrows show distorted erythrocytes when unfixed, while white arrowheads indicate a fibrous structure that is more evident prior to fixation. The similarity of the aggregates seen here (d) to the structure of fixed chitosan–GP gels (Fig. 2d) suggests that these aggregates were aldehyde-fixed chitosan microspheres. E = erythrocyte; CA = chitosan aggregates.

more than 1,500 mOsm/kg, nearly five times physiological values (Chernecky and Berger, 2004). With lower fixative concentrations (Fixative no. 3: 2% w/v paraformaldehyde in Fig. 3c, and Fixative no. 5: 2% w/v glutaraldehyde in Fig. 3d) erythrocyte distortion was reduced, retaining a quasi-biconcave in shape, for samples that were washed in aqueous saline. Erythrocyte morphology was particularly well preserved in both 5% (data not shown) and 2% w/v glutaraldehyde (Fig. 3d) where globally, the erythrocytes kept their original morphology.

Unfixed Chitosan–GP/Blood Clots and the Influence of Fixatives on Chitosan–GP/Blood Clots. Unfixed chitosan–GP/blood clots were more physically stable than blood-only clots but nonetheless suffered irreparable and rapid loss of the initial macrostructure during processing and imaging. Images of unfixed chitosan–GP/blood clot washed in 10 mM NaCl (Fig. 4a) revealed a heterogenous structure where erythrocytes (more or less distorted; white arrows in Fig. 4a) and fibrous structures (white arrowheads in Fig. 4a) could be identified. Aldehyde fixation of chitosan–GP/blood clots permitted the visualization of distinct morphologies for erythrocytes, fibres, and chitosan-specific aggregated structures (Figs. 4b–4d). A complex network of filaments appeared to connect the red blood cells that themselves exhibited a normal biconcave morphology ("E" in Figs. 4b–4d). Erythrocyte morphology was generally well preserved in chitosan–GP/blood clots for all fixatives irrespective of osmotic pressure (Figs. 4b–4d) although occasional distorted erythrocytes could be found. In general, erythrocytes were less distorted and displayed more preserved physiological features in chitosan–GP/blood clots compared with whole blood clots, when fixed and washed in the same conditions (Fig. 4 vs. Fig. 3). This is an indication that chitosan–GP com-

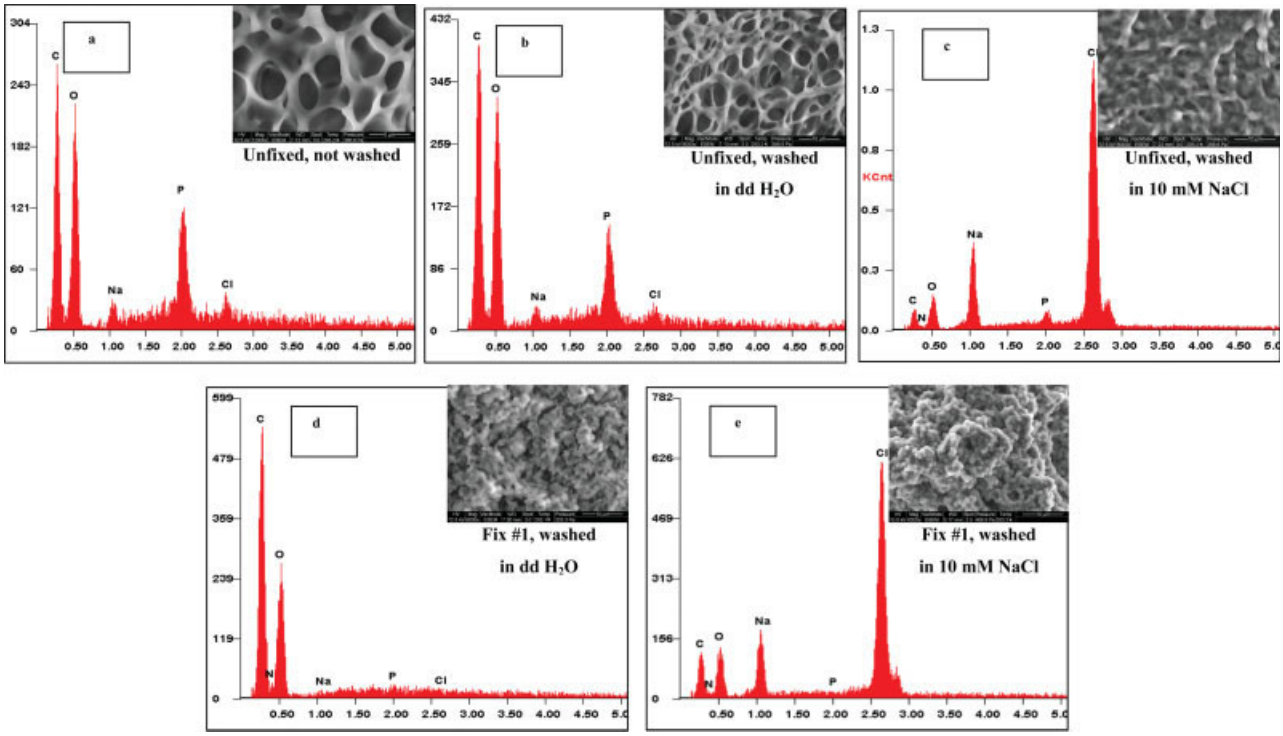

Fig. 5. Large scale EDS spectra recorded on (**a**) unfixed chitosan–GP gels that were not washed and (**b**) washed with ddH_2O and (**c**) washed with 10 mM NaCl and (**d**) chitosan–GP gels fixed with 4% w/v paraformaldehyde + 1% w/v glutaraldehyde (Fixative no. 1 in Table 1) and washed with ddH_2O or (**e**) washed in 10 mM NaCl. The reduction in phosphate peak with fixation and washing is evidence that the majority of glycerol phosphate is freely diffusing rather than being bound to chitosan. The scanned EDS analysed areas are given as ESEM insets. The y-axis units are counts per second. [Color figure can be viewed in the online issue, which is available at www.interscience.wiley.com.]

pound provides a structural and cytoprotective effect on whole blood cell components in the hybrid clot.

Chitosan-specific structures in the form of aggregates of spherical microparticles similar to those seen in fixed chitosan–GP gels were also observed in all chitosan–GP/blood clots ("CA" in Figs. 4c and 4d). The aggregates had a range of 1.2–1.8 μm in diameter and appeared homogenously distributed among the erythrocytes. The absence of these aggregates in unfixed chitosan–GP/blood clots (Fig. 3a) and the similarity of these aggregates to the structure of fixed chitosan–GP gels (Fig. 2d) suggest that these aggregates were also aldehyde-fixed chitosan microspheres.

EDS Microanalysis

Global (Large Scale) Analysis. EDS spectra of all samples revealed the presence of C, O, and N as the signature of the constitutive organic material, while detected Na and Cl were a result of the salts and P was from GP. Figure 5 illustrates the global EDS spectra obtained from chitosan–GP-only gels unfixed and unwashed (a), washed with water (b) and 10 mM NaCl (c), and fixed with Fixative no. 1: 4% w/v paraformaldehyde + 1% w/v glutaraldehyde and washed with the same solutions (d, e), respectively. The scanned analyzed areas are given in insets (Figs. 5a–5e). Quantitative EDS revealed a significant depletion in phosphorous consistent with diffusive loss from 3.6 to 2.4% for unfixed and unwashed chitosan–GP gel (Fig. 5a) after washing in water (Fig. 5b), or 1.4% after washing in 10 mM NaCl (Fig. 5c). Fixed chitosan–GP samples washed either with water-only or 10 mM NaCl only allowed small amounts, 0.1 to 0.2%, of phosphorous to be detected (Figs. 5d and 5e). The lower level of GP after NaCl washing compared with washing with water is due to the ability of Cl to exchange with GP and still maintain electro-neutrality of the gel. The even lower content of GP in fixed gels is due to diffusive loss into the fixation solution. The above results indicate that the majority of GP is not bound to chitosan but is freely diffusible, so that ionic cross-linking of chitosan by GP is unlikely as a gelation mechanism.

Local (Spot) EDS Analyses. As described above (in Unfixed Chitosan–GP Gels and the Effect of Fixatives on Chitosan–GP Gel Ultrastructure and Unfixed Chitosan–GP/Blood Clots and the Influence of Fixatives on Chitosan–GP/Blood Clots) we observed aggregates of chitosan microparticles 1.2–1.8 μm in diameter after fixing chitosan–GP gels and chitosan–GP/blood clots in either paraformaldehyde or glutaraldehyde. To assess whether the observed microparticle aggregates in the chitosan–GP/blood clots were precipitates of chitosan, we performed local EDS on these structures. Figure 6 shows ESEM micrographs and EDS spectra of a chitosan aggregate from a fixed chitosan–GP gel (a) and on a microparticle aggregate feature seen in a fixed chitosan–GP/blood clot (b) where both samples were fixed

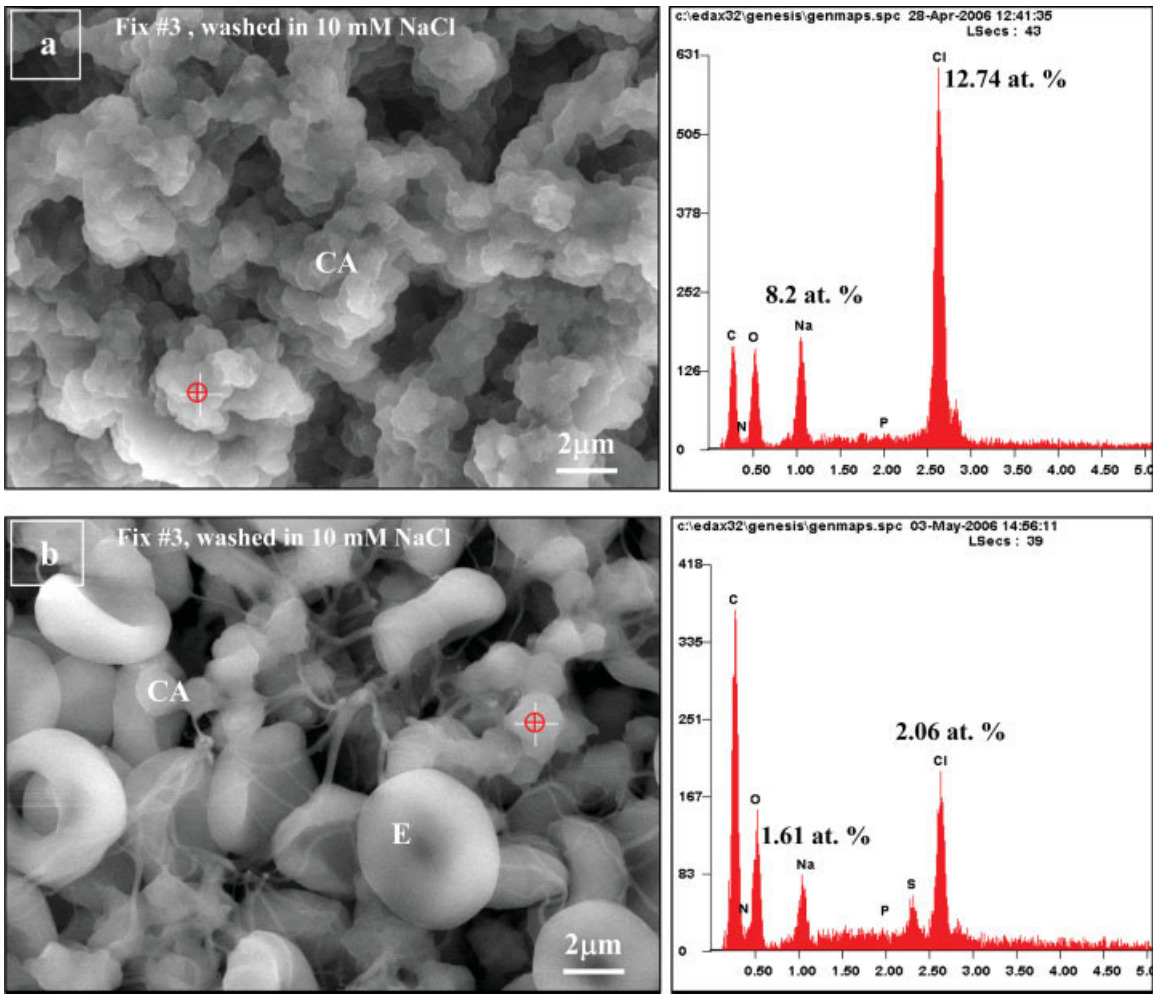

Fig. 6. ESEM micrographs and EDS spectra taken at 5 KV at the locations indicated by the symbol "⊕"in micrographs from (**a**) a chitosan aggregate (CA and ⊕) in a fixed chitosan–GP gel and (**b**) a spheroid-like feature that is also chitosan aggregate (CA and ⊕) seen in a fixed chitosan–GP/blood clot. Samples were fixed with 2% w/v paraformaldehyde (Fixative no. 3 in Table 1) and washed with 10 mM NaCl aqueous solution. A Cl/Na ratio > 1 in EDS spectra at ⊕ indicate cationic chitosan attracting a local excess of Cl vs Na. E = erythrocyte; CA = chitosan aggregates. X-rays were acquired from a pear-shaped volume for which the in-plane projected area equals that of symbol "⊕" in micrographs (size below 500 nm). The *y*-axis units are counts per seconds. [Color figure can be viewed in the online issue, which is available at www.interscience.wiley.com.]

with 2% paraformaldehyde and then washed with 10 mM NaCl. Quantitative analyses of these EDS data revealed a higher content of Cl compared with Na in these features. The ratio of Cl to Na in chitosan–GP-only aggregates was 1.55, compared with 1.28 in the case of the microparticle aggregate from the chitosan–GP/blood sample. The excess Cl compared with Na after washing with 10 mM NaCl indicates the presence of cationic chitosan that attracted chloride counterions and repelled sodium co-ions as in Donnan equilibrium (Donnan, 1911) and can be used to identify chitosan. The lower Cl/Na ratio of chitosan aggregates in chitosan–GP/blood clots versus chitosan–GP gels without blood may be due to blood proteins binding to chitosan and partially masking its cationic charge. Close examination of the spectra of other elements reveals that the aggregate in the chitosan–GP/blood has more relative carbon (about 70%) than the aggregate in chitosan–GP alone (about 56%) and contains additional sulphur (less than 0.5%) originating from other organic compounds present in blood.

When imaging chitosan–GP gels with and without blood using ESEM, micro- or nanostructured fibres were observed. To identify these fibres and distinguish between fibrin and chitosan, we carried out local EDS microanalysis after washing both unfixed and fixed samples in 10 mM NaCl, such that a Cl/Na ratio exceeding 1 (in the range of 1.2–2.4) was indicative of cationic chitosan and a ratio close to 1 (below 1.2) indicated fibrin. EDS/ESEM data were obtained from various sites (red crosses in Fig. 7) on chitosan–GP/blood clots washed in 10 mM NaCl solution, and showed that both fibres in an unfixed chitosan–GP/blood clot (CF in Fig. 7a) and in a fixed chitosan–GP/blood clot (CF in Fig. 7b) contain chitosan since EDS analyses revealed a Cl/Na atomic ratio of 1.42 (±10%) and 1.3 (±10%), respectively. Interestingly, the morphology of unfixed thick fibres (CF in Fig. 7a) seen in chitosan–GP blood

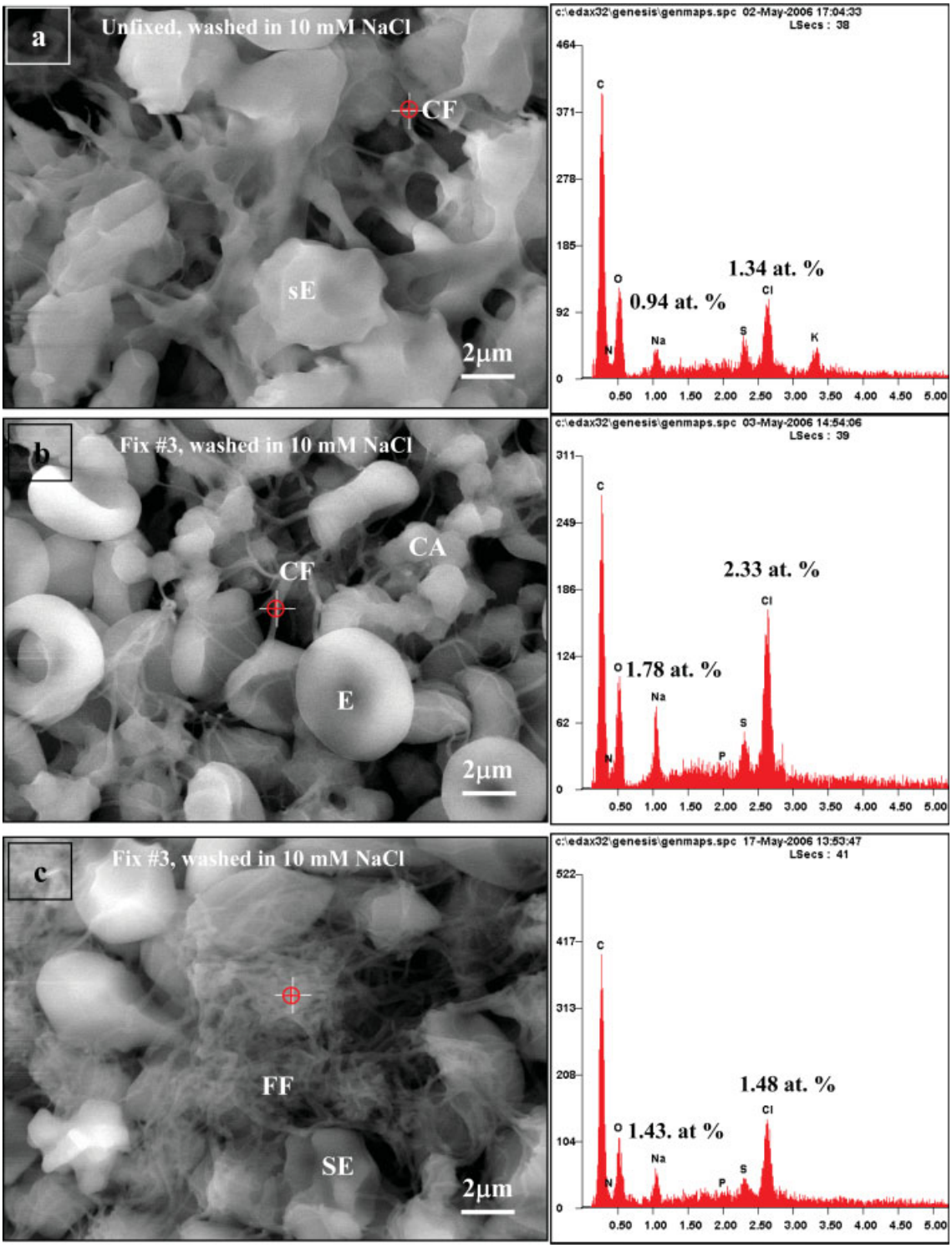

Fig. 7. ESEM micrographs and EDS spectra taken at 5 kV at the locations indicated by the symbol "⊕" in micrographs of (**a**) unfixed chitosan–GP/blood clot that contain thick chitosan fibres (CF and ⊕) and (**b**) chitosan–GP/blood clot fixed with 2% w/v paraformaldehyde (Fixative no. 3) that contain thin chitosan fibres (CF and ⊕) and (**c**) a blood only clot fixed with 2% w/v paraformaldehyde (Fixative no. 3 in Table 1) containing a filamentous fibrin network (FF and ⊕). All samples were washed in 10 mM NaCl aqueous solution. Identification of chitosan fibres (CF) vs. FF was by the Cl/Na ratio ≈ 1.3 for CF vs. 1.0 for FF. E = erythrocyte; sE = shrunken erythrocyte; CA = chitosan aggregates; CF = chitosan fibres, and FF = fibrin fibres. X-rays are acquired from a pear-shape volume of which the in-plane projected area equals that of symbol "⊕" in micrographs (size below 500 nm). The *y*-axis units are counts per seconds. [Color figure can be viewed in the online issue, which is available at www.interscience.wiley.com.]

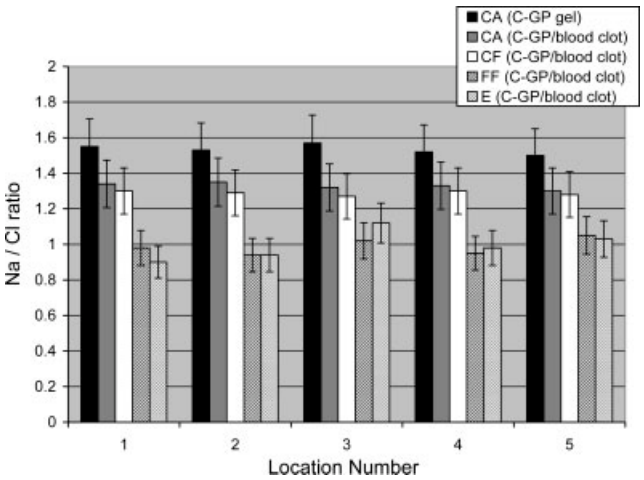

Fig. 8. Cl/Na ratios of chitosan aggregates (CA) in chitosan–GP gels, and chitosan aggregates (CA), chitosan fibres (CF), fibrin fibres (FF) and erythrocytes (E) distinguished in chitosan–GP/blood clots fixed with 4% w/v paraformaldehyde + 1% w/v glutaraldehyde (Fixative no. 1 in Table 1) and washed with 10 mM NaCl, in five distinct locations (labelled from 1 to 5 on the *x*-axis) taken from the middle of clots. Chitosan fibres were distinguished from fibrin fibres by an excess of Cl compared with Na in the former, after washing with 10 mM NaCl, due to the cationic nature chitosan attracting chloride counter-ions and repelling sodium co-ions. Error bars are ±10% of the actual Cl/Na ratio value for each feature and location.

clots resembles the mesh-like network morphology of unfixed chitosan–GP gels (Fig. 2c). This further supports the evidence that chitosan microparticle aggregates seen in fixed chitosan GP/blood clots are artefacts (CA in Figs. 4c and 4d). Conversely the dense, fine filamentous structures preponderantly observed in paraformaldehyde-fixed blood-only clots are fibrin fibres (FF in Fig. 7c), and are consistent with the EDS quantification providing nearly equal amounts of Cl and Na.

Direct comparison of Cl/Na ratios obtained by EDS from various features in specimens fixed with 4% w/v paraformaldehyde + 1% w/v glutaraldehyde and washed with 10 mM NaCl were consistent with their identification as chitosan aggregates (CA) in chitosan–GP gels, and CA, chitosan fibers (CF), fibrin fibers (FF), and erythrocytes (E) in chitosan–GP/blood clots (Fig. 8). We found these features to provide Cl/Na ratios that were independent of location and that only chitosan-containing structures exhibited excess Cl compared with Na after washing with 10 mM NaCl. This local EDS analysis was mainly used to distinguish chitosan fibres from fibrin fibres.

To summarize, extensive networks of fibres are observed in both blood-only and chitosan–GP/blood clots. These networks were particularly clear in unfixed samples, although unfixed blood-containing samples were technically challenging to image in ESEM. In blood-only samples, fibres were assumed to be fibrin fibres polymerised during coagulation while fibres of different types were observed for the chitosan–GP/blood clots that were both blood-derived (fibrin) and chitosan-derived according to EDS analyses.

CONCLUSIONS

The main objective of this study was to characterize the structure and interactions of the various components of chitosan–GP/blood clots compared with those of chitosan–GP gels and whole blood clots. We have exploited the principal advantage of ESEM of allowing investigation of hydrated samples, as applied to chitosan–GP/blood clots to permit observation of ultrastructure under close to physiological conditions. The main conclusions of this study are:

1. Chitosan–GP/blood clots contain morphologically normal erythrocytes and a fibrous network derived from both chitosan and coagulation-dependent fibrin formation.
2. Chitosan–GP gels form an open porous network composed of chitosan where GP is unbound and freely diffusible as indicated by its depletion into fixation or wash solutions.
3. Fixation of chitosan-containing materials with aldehydes produced structural artefacts. In this study aldehyde fixatives modified the morphology of chitosan–GP gels from an initial mesh-like network to a more condensed structure containing aggregates of chitosan microparticles of ~1.5 μm diameter. Similar aggregates were observed in fixed chitosan–GP/blood clots.
4. Washing with 10 mM NaCl prior to ESEM imaging and EDS permits the identification of concentrated cationic structures such as chitosan through high Cl to Na atomic ratios. We used this method to demonstrate that the aldehyde-induced microparticle precipitates are chitosan and to distinguish chitosan-containing structures from other structures in chitosan–GP blood clots.
5. All the fixatives tested in this study, except hypertonic 4% w/v paraformaldehyde (Fixative no. 2), preserved acceptable erythrocyte morphology.

ACKNOWLEDGMENTS

Salary support for CH was provided by the Fonds de la Recherche en Santé Quebec (FRSQ).

REFERENCES

Buckwalter JA, Mankin HJ. 1998. Articular cartilage repair and transplantation. Arthritis Rheum 41:1331–1342.

Chenite A, Chaput C, Wang D, Combes C, Buschmann MD, Hoemann CD, Leroux JC, Atkinson BL, Binette F, Selmani A. 2000. Novel injectable neutral solutions of chitosan form biodegradable gels in situ. Biomaterials 21:2155–2161.

Chenite A, Buschmann M, Wang D, Chaput C, Kandani N. 2001. Rheological characterisation of thermogelling chitosan/glycerol-phosphate solutions. Carbohydr Polym 46:39–47.

Chernecky CC, Berger BJ, editors. 2004. Laboratory tests and diagnostic procedures, 4th ed. Philadelphia: Saunders.

Chevrier A, Hoemann CD, Sun J, Buschmann MD. 2006. Chitosan glycerol phosphate-blood implants increase cell recruitment, transient vascularisation and subchondral bone remodeling in drilled cartilage defects. Osteoarthritis Cartilage 15(3):316–327.

Clark RAF. 1996. The molecular and cellular biology of wound repair. New York: Plenum Press.

Cohen I, Gerrard JM, White JG. 1982. Ultrastructure of clots during isometric contraction. J Cell Biol 93:775–787.

Colman RW, Hirsh J, Marder VJ, Clowes AW, George FN, editors. 2001. Hemostasis and thrombosis: Basic principles and clinical practice. Philadelphia: Lippincott Williams and Wilkins.

Crompton KE, Prankerd RJ, Paganin DM, Scott TF, Horne MK, Finkelstein DI, Gross KA, Forsythe JS. 2005. Morphology and gelation of thermosensitive chitosan hydrogels. Biophys Chem 117:47–53.

Danilatos GD. 1981a. Design and construction of an atmospheric or environmental SEM. Scanning 4:9–20.
Danilatos GD. 1981b. The examination of fresh or living plant-material in an environmental scanning electron-microscope. J Micro (Oxford) 121:235–238.
Danilatos GD. 1983. A gaseous detector device for an environmental SEM. Micron Micro Acta 14:307–318.
Donnan FG. 1911. Theory of the balances of membranes and potential of membranes at the existence of non dialysing electrolytes—A contribution to physical chemical physiology. Z Elektrochem Angew Phys Chem 17:572–581.
Filion D, Lavertu M, Buschmann MD. 2007. Ionisation and solubility of chitosan solutions related to thermosensitive chitosan/glycerol-phosphate systems. Biomacromolecules 8:3224–3234.
Hayat MA. 2000. Principles and techniques of electron microscopy: Biological applications. Cambridge: Cambridge University Press.
Hoemann CD, Sun J, Légaré A, McKee MD, Buschmann MD. 2005a. Tissue engineering of cartilage using an injectable and adhesive chitosan-based cell-delivery vehicle. Osteoarthritis Cartilage 13:318–329.
Hoemann CD, Hurtig M, Rossomacha E, Sun J, Chevrier A, Shive MS, Buschmann MD. 2005b. Chitosan-glycerol phosphate/blood implants significantly improve hyaline cartilage repair in ovine microfracture defects. J Bone Joint Surg 87A:2671–2686.
Hoemann CD, Sun J, McKee MD, Chevrier A, Rossomacha E, Rivard GE, Hurtig MB, Buschmann MD. 2006. Chitosan-glycerol phosphate/blood implants elicit hyaline cartilage repair integrated with porous subchondral bone in microdrilled rabbit defects. Osteoarthritis Cartilage 15:78–89.
Hoemann CD, Chenite A, Sun J, Serreqi A, Hurtig M, Lu Z, Rossomacha E, Buschmann MD. 2007. Cytocompatible gel formation of chitosan-glycerol phosphate solutions supplemented with hydroxyl ethyl cellulose is due to the presence of glyoxal. J Biomed Mater Res A 83:521–529.
Hunter EE. 1993. Practical electron microscopy: A beginner's illustrated guide. Cambridge: Cambridge University Press.
Lavertu M, Filion D, Buschmann MD. 2007. Heat-induced transfer of protons from chitosan to glycerol phosphate produces chitosan precipitation and gelation. Biomacromolecules, accepted.
Leong ASY. 1994. Fixation and fixatives. Woods AE, Ellis RC, editors. Laboratory Histopathology: A Complete Reference. London: Churchill Livingstone, 4:1–26.
Morgenstern E, Ruf A, Patscheke H. 1990. Ultrastructure of the interaction between human platelets and polymerizing fibrin within the first minutes of clot formation. Blood Coagul Fibrinolysis 1:543–546.
Muscariello L, Rosso F, Marino G, Giordano A, Barbarisi M, Cafiero G, Barbarisi A. 2005. A critical overview of ESEM applications in the biological field. J Cell Physiol 205:328–334.
Rizzieri R, Baker FS, Donald AM. 2003. A study of the large strain deformation and failure behaviour of mixed biopolymer gels via in situ ESEM. Polymer 44:5927–5935.
Sheehan D, Hrapchak B, editors. 1987. Theory and practice of histotechnology. Columbus: Battelle Press.
Stokes DJ. 2003. Recent advances in electron imaging, image interpretation and applications: Environmental scanning electron microscopy. Phil Trans R Soc Lond A 361:2771–2787.
Stokes DJ, Rea SM, Best SM, Bonfield W. 2003. Electron microscopy of mammalian cells in the absence of fixing, freezing, dehydration, or specimen coating. Scanning 25:181–184.
Tallheden T, Dennis JE, Lennon DP, Sjögren-Jansson E, Caplan AI, Lindahl A. 2003. Phenotypic plasticity of human articular cartilage. J Bone Joint Surg 85A (Suppl. 2):93–100.
White JG. 2000. Platelet secretion during clot retraction. Platelets 11:331–343.
Zan J, Chen H, Jiang G, Lin Y, Ding F. 2006. Preparation and properties of crosslinked chitosan thermosensitive hydrogel for injectable drug delivery systems. J Appl Polym Sci 101:1892–1898.